Journal of Membrane Science Letters 4 (2024) 100072

Contents lists available at ScienceDirect

Journal of Membrane Science Letters

journal homepage: www.elsevier.com/locate/memlet

# Impact of surfactants on membrane fouling during separation of an oil-water emulsion

Xu Yu [a], Naama Segev [a], Kirti Sankhala [b,1], David Jassby [c], Eric M.V. Hoek [c], Guy Z. Ramon [a,b,*]

[a] Department of Civil & Environmental Engineering, Technion - Israel Institute of Technology, Haifa 3200003, Israel
[b] Wolfson department of Chemical Engineering, Technion - Israel Institute of Technology, Haifa 3200003, Israel
[c] Department of Civil & Environmental Engineering, University of California - Los Angeles (UCLA), Los Angeles 90095, United States

ARTICLE INFO

*Keywords:*
Membrane separaion
Oil-water emulsion
Surfactants
fouling
Direct observation

ABSTRACT

While membrane separation has proven to be an outstanding method for separating oil in water (O/W) emulsions containing droplets smaller than 20 μm, it is severely limited due to fouling. Much research has been aimed at understanding the mechanism behind membrane fouling, particularly for ultrafiltration (UF) membranes. Interestingly, studies pointed out that the emulsifier, namely surfactant, is the main source of fouling in nanofiltration and reverse osmosis, while in the case of UF, oil is generally regarded as the main source of fouling. Herein, we study the fouling of UF membranes during separation of O/W emulsions stabilized by surfactants, with the explicit goal of determining the relative impact of the oil and surfactant present on fouling severity and dynamics. Results obtained from flux decline measurements, complimented by visualization using confocal microscopy, show that oil causes irreversible fouling to a certain extent, however, surfactant fouling dominates the observed membrane performance. The degree of fouling and flux recovery appears to be closely related to the properties the surfactant, namely charge and molecular weight, as has been observed in the past but attributed to the oil-membrane interactions, mediated by the surfactant. Further, to visualize the fouling mechanisms, direct observation via a confocal microscope set-up is used to capture real-time images of the membrane surface, which reveal that surface coverage of oil is not directly related to flux decline during the separation process. Our results suggest that membrane flux decline and fouling is dominated by membrane-surfactant interactions, the exact nature of which is a topic for future extensions of this work.

## Introduction

Oily wastewater is generated by many industries, e.g., shale oil and gas, petrochemical, metallurgical, food, and pharmaceutical industries (Hu et al., 2013; Ahmad et al., 2020; Padaki et al., 2015; EPA, 2002; Yu et al., 2017; Kalla, 2021). Traditional treatment by froth-flotation and coagulation flocculation cannot separate stabilized O/W emulsions, where droplet size is <20 μm (Finborud et al., 1999; Zhao et al., 2021; Lapointe and Barbeau, 2020). Offering fit-for-purpose tunability, easy operation, low energy consumption and efficient separations (Adhikari and Fernando, 2006; Ismail et al., 2009), membrane filtration has become of increasing interest in the past few decades, and is broadly applied in treating oily wastewater streams, especially stable O/W emulsion (Qiao et al., 2008; Madwar and Tarazi, 2003; Çakmakce et al., 2008; Kim et al., 2011). However, membranes often suffer from severe fouling, which affects process energy consumption and costs. A key step for fouling mitigation lies in understanding the mechanisms of fouling formation. However, the influence of surfactants on fouling during stable O/W emulsion separation remains elusive. Several studies have assumed that adsorption of charged surfactant onto both the membrane surface and the oil droplet can effectively prevent interaction between the oil and the membrane surface due to electrostatic repulsion (Wu et al., 2018). Meanwhile, for the case of nanofiltration and reverse osmosis membranes, it has been pointed out that surfactants are the main foulants due to strong surfactant adsorption in/onto the membrane pores (Virga et al., 2021; Chen et al., 2016). Nevertheless, reports on surfactant fouling of porous membranes with molecular weight cut-off (MWCO) larger than the surfactant, particularly ultrafiltration (UF)

* Corresponding author.
*E-mail address:* ramong@technion.ac.il (G.Z. Ramon).
[1] Currrent affiliation: Center for Emerging Technologies for Sustainable Development (CETSD), Indian Institute of Technology Jodhpur, Karwar, Jodhpur 342037 Rajasthan, India.

https://doi.org/10.1016/j.memlet.2024.100072
Received 12 January 2024; Received in revised form 26 February 2024; Accepted 26 February 2024
Available online 3 March 2024

membranes, are few and evidence remains inconclusive.

To date, most of the studies use indirect measurement to understand the fouling on UF membranes during the emulsion separation process. Through changing the working parameters such as transmembrane pressure (TMP), temperature, pH, surfactant concentration and oil concentration, the permeate flux of the membrane is changed, hence indicating a mitigation or alleviation of membrane fouling. Direct observation of the membrane via confocal microscopy, providing real-time images of oil deposition on the membrane has been shown proved to be a useful approach to monitor the dynamics of oil droplets on the membrane surface (Vu et al., 2019; Dickhout et al., 2018; Fux and Ramon, 2017), as well as providing a means to understand the influence of anti-fouling surface modifications (Itzhak et al., 2021).

In the present study, we investigated the relative impact of the main constituents of the emulsion, namely the oil droplets and the surfactant, on fouling of UF membranes. In particular, we use both 'bulk' flux decline experiments, typically employed for fouling studies, as well as complementary in-situ visulization using a high-resolution confocal microscopy setup.

## Materials and methods

### *Membranes and feed composition*

Commercially available polyethersulfone (PES) flat sheet UF membranes (Synder filtration) were used, with MWCO of 20 kDa (SM) and 100 kDa (LY), as well as MF membranes composed of cellulose acetate with a 0.1 μm nominal pore size. For the emulsions, hexadecane (99 %), the neutral surfactant triton X-100 (TX), negatively charged surfactant sodium dodecyl sulfate (SDS), and positively charged surfactant hexadecyltrimethylammonium bromide (CTAB), were used (Sigma-Aldrich Co., USA). NaCl (S D Fine-Chem Limited, India) was added to the oil-water emulsion to increase the ionic strength; Rhodamine-PEG-Pyrene (RPP) (Anatrace, OH, USA) was used in surfactant filtration test for visualization. Dye-Lite (Tracerline, USA) was used as a fluorescent marker for oil droplets.

Three types of surfactant-stabilized oil emulstions (O/S/W) were prepared, comprising 500 ppm hexadecane and 0.165 mM of a surfactant (i.e., TX, SDS or CTAB), unless stated otherwise. Hexadecane was mixed with DDI water in a homogenizer (MiniBatch D-9, MICCRA) at 11,000 rpm for 3 min, followed by addition of the surfactant; the solution was then mixed with a magnetic stirrer for 10 min. Oil droplets size was measured by a particle size analyzer (Malvern Mastersizer 2000), see Fig. S2 in the supplementary material. Surfactant in water solutions (S/W) were prepared by simply mixing surfactant and water with a magnetic stirrer for 10 min. In addition, a drop shape analyzer (DSA25E, Krüss) was used for measuring the surface tension of all the solutions and the contact angle between oil and membrane in the surfactant solution with and without NaCl. The Zeta potential of the oil droplets in the surfactant solution was measured using a Malvern Zetasizer Nano (Malvern Instruments Ltd., UK), see Fig. S2 in the supplementary material.

### *Crossflow filtration system*

A crossflow membrane filtration system was employed, with 3 identical cells (each with a total membrane filtration area of 19.5 $cm^2$). Feed was supplied from a sealed tank, pressurized by compressed air via a controller (MFCS-EZ, FLUIGENT), with trans-membrane pressure (TMP) measured by a differential pressure transducer (Omega Engineering, USA). Cross flow was maintained by a micro gear pump (see supplementary material for a schematic of the system). During a permeability test, membranes were first stabilized at a TMP of 0.5 bar for 30 mins, after which permeability tests were conducted under crossflow mode at 0.5, 1.0 and 1.5 bar. At each TMP, after stabilizing the flux for 10 min, the weight of the permeate was continuously recorded for 5 min, with an interval of 4 s. The permeate flux was calculated by converting the mass to volume and calculating the difference in volume at set time intervals. Membrane permeance was then calculated based on the linear regression of the average flux plotted against the applied pressure.

Separate visualization experiments were performed using a custom-made flowcell, providing high-resolution optical access to the membrane surface via confocal microscopy (Fux and Ramon, 2017) (see schematic illustration in Fig 1). The flowcell dimensions are 0.6 × 6 × 36 mm ($h \times w \times l$), providing an active membrane area of 2.16 $cm^2$. The system is identical to the one used for the fouling tests, except for the flowcell, which was mounted on the stage of a confocal microscope. Also, permeation was measured using a flow sensor (Fluigent). During the experiment, 3 regions, each with an area of 2 × 2 $mm$, are scanned by the confocal microscope with a step size of 0.33 μm in the vertical direction, every 5 min. The excitation/emmission wavelength of the fluorescent dye is 561 nm; reflected and fluorescent signals were used to capture the membrane surface and the dyed oil droplets, respectively. In order to obtain the aereal oil coverage, image analysis was preformed using binary pixel conversion performed in ImageJ. All visualization experiments were repeated at least twice, to ensure reproducibility of the results. Furthermore, in order to visualize the interaction of surfactant with the membrane surface, Rhodamine-PEG-pyrene (RPP) - an amphiphilic molecule, was used, where the Rhodamine is the fluorophore detectable via confocal microscopy.

### *Fouling experiments*

Filtration tests were conducted in crossflow mode. Following a permeability test, a feed solution was first circulated for 10 min with no pressure at 150 ml/min to ensure complete filling of the system. Next, the pressure was adjusted, in different experimental sets, at 0.5, 1.0, 1.5 or 2.0 bar. Permeate weight was continuously recorded during each 1hr test. The flux is expressed scaled against the pure water flux, $\overline{J} = J/J_0$, where $J$ is the water flux and $J_0$ is the initial water flux obtained through the permeability test. Following the fouling atep, a cleaning step was performed and the feed was replaced by DDI water and circulated in cross-flow mode, at 1 bar for 30 min, after which the feed was replaced with fresh DDI water and circulated in a crossflow mode, without any external pressure, for an additional 10 min. Following the membrane cleaning, membrane permeability was measured again (as detailed in Section 2.2) to assess the flux recovery.

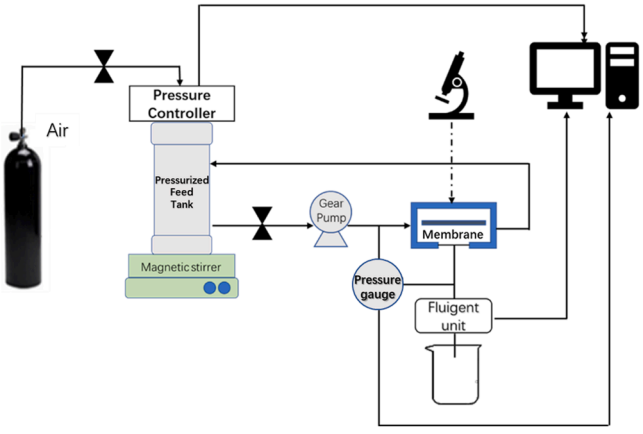


**Fig. 1.** Schematic diagram of the direct observation crossflow filtration system. A flowcell, fitted with a glass window, is placed on the stage of a confocal microscope for in-situ monitoring of the membrane surface. A pressure controller monitors the pressurized tank from which the feed stream is supplied into the cell. The permeate flux is continuously recorded by a microfluidic flow rate sensor, in conjunction with the acquired microscopic images.

## Results and discussion

### *Flux decline is mostly caused by surfactants, not oil*

We begin by examining the degree of flux decline during O/S/W separation, as presented in Fig. 2. Regardless of operating conditions and surfactant type, a clear common feature is observed, namely, that the flux decline is insensitive to the presence of oil - as long as the surfactant is present. This outcome is very repeatable, and is manifested by an insignificant difference in the final flux measured at the end of each fouling test, conducted under identical conditions with or without oil present in the feed, as shown in Fig. 2a (see supplementary material for complete data sets showing the dynamics during these tests). A similar trend is found in the direct observation experiments, in the dynamics of both flux decline and membrane area coverage (see Figs 2b-d). In the latter case, visualization clearly shows that the flux is not correlated with the degree of membrane surface coverage, most strongly exemplified for the case of an O/W mixture (without surfactant), where the membrane is nearly completely covered in oil, while the flux decline is much smaller than that observed in the presence of the surfactants. While the severity of flux decline does change with the type of surfactant employed, the presence or absence of oil makes very little difference, up to oil concentrations of 5000 ppm (see supplementary material, Fig. S6).

In general, charge interactions are expected to be present between the oil droplets and the membrane, which become screened as the ionic strength is increased, or when a non-ionic surfactant is used (these effects have already been observed in the literature (Dickhout et al., 2018; Tummons et al., 2017), which has been focused on the oil-membrane interactions). However, this is mostly manifested by the reversibility of oil coverage, and not so much in terms of flux recovery, which is apparently dependent on other, surfactant-specific factors, possibly molecular size, hydrophobic interactions and surfactant-surfactant interactions (increasing the concentration of the surfactant results in a much greater degree of flux decline). Differences in droplet behavior in the presence of charged vs. uncharged surfactants are apparent in the severity of flux decline, but more interestingly, in the degree of membrane coverage and, at least qualitatively, the morphology of the oil layer. This is likely an interesting outcome of membrane-oil interactions modulated by the surfactant type, and is also manifested in the degree of flux recovery after rinsing (as seen in Figs 2(b-d) and summerised in Fig S3 in the supplemetal material). These aspects, however, extend beyond the scope of the current work and are left for future elaboration.

### *Membrane pore size effect on the relative impact of oil on fouling*

To further inspect the relative impact of surfactants on fouling, separation of O/S/W and S/W feed was also conducted using membranes with larger pore size, namely a 100 kDa UF membrane (LY) and a MF membrane with a nominal pore size of 0.1μm. As before, fouling was followed by a rinsing stage using DI water (see Fig. 3). The results show the flux decline with and without oil, alongside real-time confocal images. For the 100 kDa UF membrane and a TX solution, rapid flux decline is observed, with or without the presence of oil. Meanwhile, filtration of a feed containing only water and oil exhibited much lower flux decline over the same experimental duration. As before, the presence of surfactant affects reversibility - a simple water rinse recovers much of the flux in the cases where TX was present, whereas the flux of a membrane exposed to oil alone is not as affected by DI rinsing. In contrast, for the MF membrane, the flux decline behavior is qualitatively different. While all three cases foul the membrane, the combination of oil and surfactant

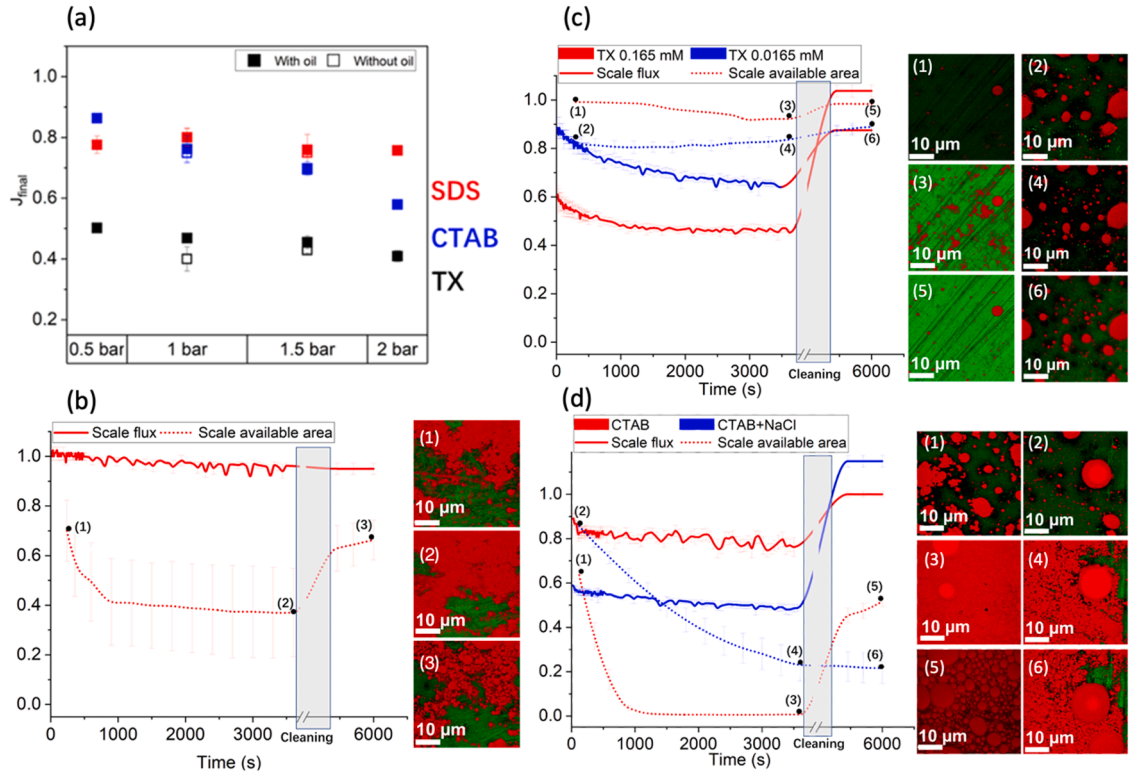


**Fig. 2.** (a) Degree of flux loss, scaled against the initial flux, after 60 mins of filtration, for oil-water-surfactant (O/S/W) emulsions containing different surfactants, or without surfactant. In all these experiments, the membrane used was the SM (20 kDa), PES UF membrane. Note the overlap between the empty (no oil) and full markers (with oil) in some of the data points. (b)-(d): Flux decline during filtration experiments, along with confocal images obtained at $t = 5$ and 60 min, and following a 10 min DI water rinsing. Plots show the scaled flux and available membrane area vs filtration time, for: (b) O/W emulsion with no surfactant added (c) O/S/W emulsion with TX (concentrations of 0.165 mM and 0.0165 mM). (d) O/S/W emulsion with CTAB (0.165 mM) with and without 133 mM NaCl. All experiments were conducted at 1 bar and oil concentration was 500 ppm. The scale bar represents 10 μm.

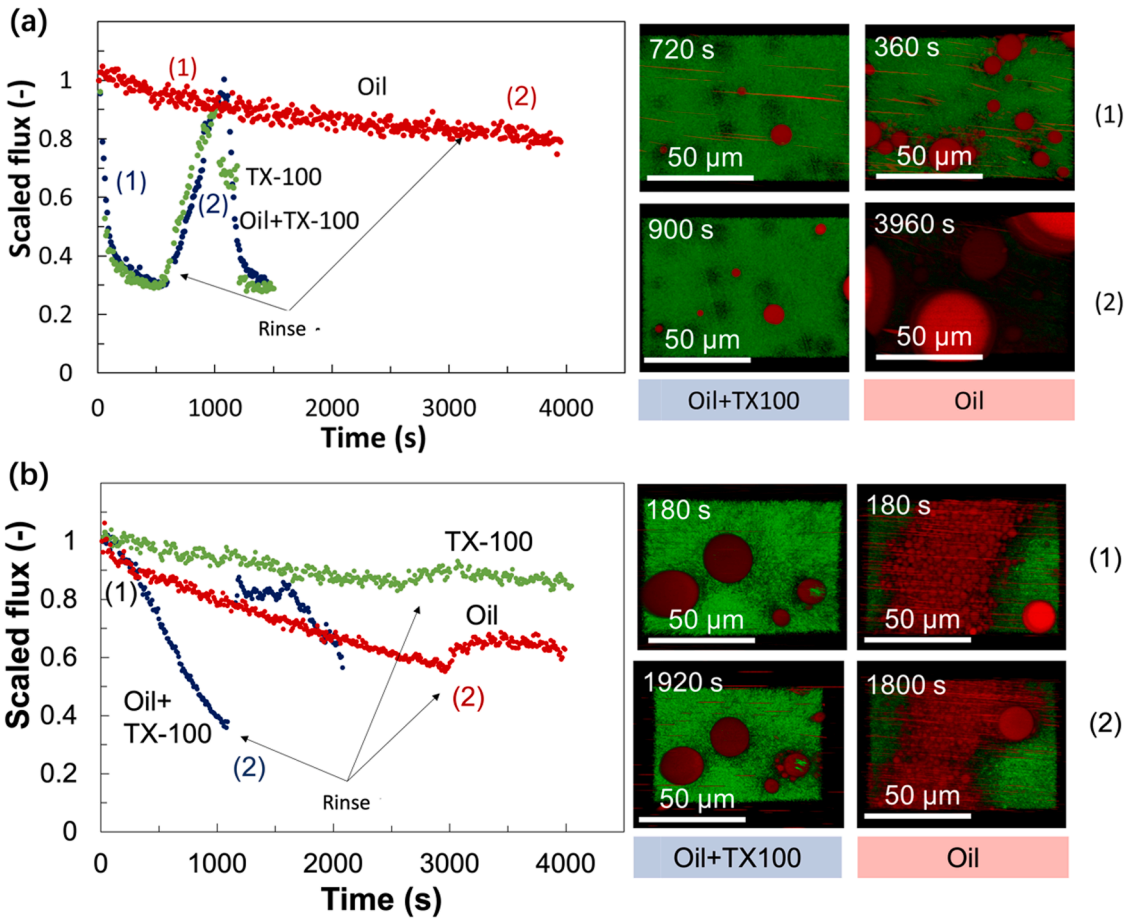


**Fig. 3.** The relative impact of oil droplets on fouling, as affected by membrane pore size. Plots show scaled flux data alongside confocal images taken during experiments separating different feed solutions: an emulsion of oil and TX-100 (blue), only oil (red) and only TX-100 (green), using 2 different membranes: (a) 100 kDa UF (initial flux ~150 LMH) and (b) MF (initial flux ~125 LMH). Points where DI water rinsing is initiated are indicated with an arrow.

is the most severe. Comparing 'only oil' with 'only TX', it seems that size plays an important role since large droplets block the membrane pores more than the small TX molecules. Rinsing the membrane with water achieves some flux recovery. Further, it appears that the presence of TX facilitates more severe, less reversible membrane fouling, presumably due to screening of electrostatic interactions. These result illustrate how, as pore sizes become comparable with oil droplet size, the contribution of oil to flux decline becomes more important.

*Internal fouling of surfactant via adsorption onto the membrane pore surface*

In the fouling visualization experiments, the oil was observable due to the addition of a fluoresecent dye, but we could not directly image the impact of the surfactants used. Therefore, in order to obtain evidence of surfactant and membrane interactions, Rhodamine-PEG-pyrene (RPP) was used in separate imaging experiments, as shown in Fig. 4. This imaging is shown alongside measurements demonstrating the degree to which the membrane rejected TX100. As demonstrated in Fig. 4, after permeation of a solution containing RPP the membrane structure can be clearly imaged throughout its depth. This indicates the penetration of RPP molecules through the membrane with at least some retained inside the pores. A reasonable conclusion is that surfactant accumulates on the surface and within the membrene pores.

TX rejection tests, as described in Section 2.2, were conducted to further assess the degree to which surfactant accumulates within the membrane structure (see Fig. 4). The concentration of TX is represented as the normalized absorption, which is the ratio between the absorption peak of TX in a tested permeate sample and the absorption measured in the feed solution. As may be seen, the surfactant passage through the MF membrane is reduced in the beginning of the experiment but becomes complete at some point. In the case of 100 kDa UF membrane, however, the rejection is very high throughout the duration of the experiment, which supports the notion of surfactant adsorprion, within the membrane porous structure, as being the cause of the observed flux decline.

## Concluding remarks

Understanding the interplay between the characteristics of oil emulsions and the membranes used to seprate them is important for better process implementation. Here, we focus on a specific aspect of this system, and examine the relative role of the emulsion constituents - oil and surfactant - in the observed flux reduction. Macroscopic flux decline measurements are aided by direct visualization using high-resolution, in-situ confocal microscopy. Our results highlight the mostly overlooked role of the surfactants as the cause for flux decline. Specifically, for membranes where, in general, the oil droplet size is larger than the membrane pore sizes, the main contributor to fouling is the surfactant, not the oil. While the severity of the fouling, in this case, is dependent on surfactant type and solution composition, this general observation is consistent. In contrast, as pore size becomes comparable to oil droplet size, the relative contribution of the oil increases, and the influence of surfactants on the contribution of oil droplets to fouling becomes apparent, manifested as variations in fouling severity and reversibility. A question arising out of the reported results is how do surfactant-membrane interactions cause such severe fouling in some cases,

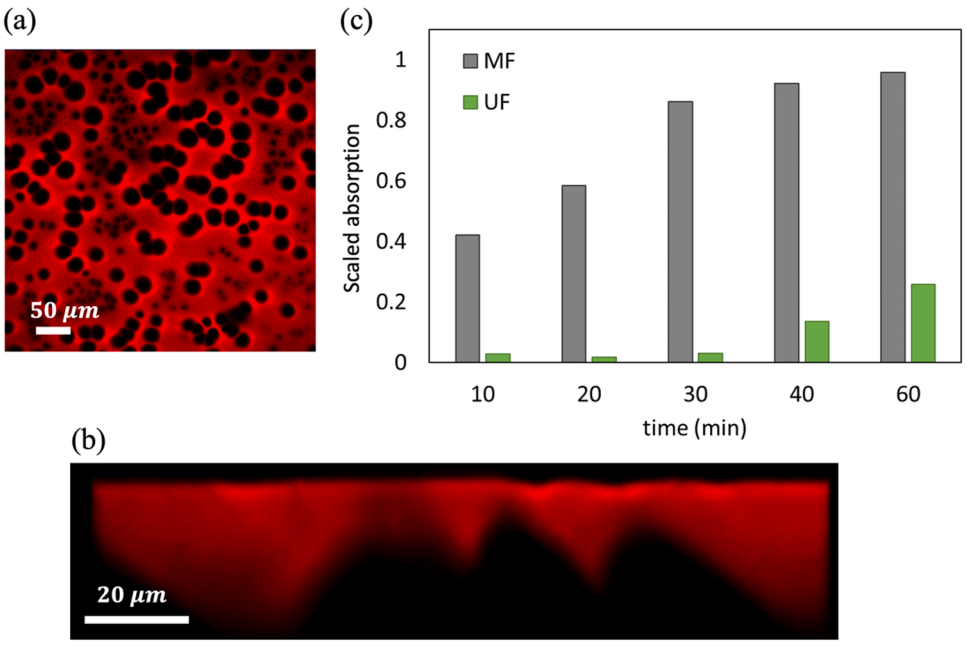


**Fig. 4.** Surfactant adsorption onto the membrane internal pore structure (SM, 20 kDa UF membrane). (a) Confocal scan, 15 μm into the membrane, of the fluorescent-labeled surfactant RPP. (b) Cross-sectional confocal reconstruction of the membrane after 60 mins of operation, showing the distribution of the fluorescent-labeled surfactant, RPP. (c) Spectrophotometric absorbance measurements, scaled against the absorbance in the bulk solution, of TX-100 in the permeate during separation using the UF (LY, 100 kDa) and MF membranes, illustrating 'breakthrough' behavior.

despite the comparatively small molecular size. This interesting point is left for future research.

## Supplemental information

Details of characterization of emulsions and membranes, including oil droplet diameters, surface tension of air/solution and oil/solution, zeta potential of the surfactant solution, oil rejection of the membrane, and contact angle between oil and the membrane in the circumstance of surfactant solution; flux measurement during the fouling experiments;

## CRediT authorship contribution statement

**Xu Yu:** Writing – review & editing, Writing – original draft, Visualization, Formal analysis, Data curation. **Naama Segev:** Writing – original draft, Visualization, Formal analysis, Data curation. **Kirti Sankhala:** Writing – original draft, Investigation. **David Jassby:** Writing – review & editing, Project administration, Investigation. **Eric M.V. Hoek:** Writing – review & editing, Project administration, Investigation. **Guy Z. Ramon:** Writing – review & editing, Writing – original draft, Visualization, Supervision, Investigation, Funding acquisition, Conceptualization.

## Declaration of competing interest

The authors declare the following financial interests/personal relationships which may be considered as potential competing interests: Guy Ramon reports financial support was provided by United States-Israel Binational Science Foundation. David Jassby reports financial support was provided by National Science Foundation. Eric Hoek reports financial support was provided by National Science Foundation. If there are other authors, they declare that they have no known competing financial interests or personal relationships that could have appeared to influence the work reported in this paper.

## Data availability

No data was used for the research described in the article.

## Acknowledgments

The research was supported by the US-Israel binational Science foundation (BSF) grant number 2019603.

## Supplementary materials

Supplementary material associated with this article can be found, in the online version, at doi:10.1016/j.memlet.2024.100072.

## References

Adhikari, S., Fernando, S., 2006. Hydrogen membrane separation techniques. Ind. Eng. Chem. Res. 45, 875–881.
Ahmad, T., Guria, C., Mandal, A., 2020. A review of oily wastewater treatment using ultrafiltration membrane: a parametric study to enhance the membrane performance. J. Water Process Eng. 36, 101289.
Çakmakce, M., Kayaalp, N., Koyuncu, I., 2008. Desalination of produced water from oil production fields by membrane processes. Desalination 222, 176–186.
Chen, D., Zhao, X., Li, F., Zhang, X., 2016. Influence of surfactant fouling on rejection of trace nuclides and boron by reverse osmosis. Desalination 377, 47–53.
Dickhout, J.M., Kleijn, J.M., Lammertink, R.G.H., De Vos, W.M., 2018. Adhesion of emulsified oil droplets to hydrophilic and hydrophobic surfaces-effect of surfactant charge, surfactant concentration and ionic strength. Soft Matter 14, 5452–5460.
U. EPA, Development Document for Final Effluent Limitations Guidelines and Standards for the Iron and Steel Manufacturing Point Source Category, (2002).
Finborud, A., Faucher, M., Sellman, E., 1999. New method for improving oil droplet growth for separation enhancement. In: SPE Annual Tech. Conference Exhibition, Society of Petroleum Engineers.
Fux, G., Ramon, G.Z., 2017. Microscale dynamics of oil droplets at a membrane surface: deformation, reversibility, and implications for fouling. Environ. Sci. Technol. 51, 13842–13849.
Hu, G., Li, J., Zeng, G., 2013. Recent development in the treatment of oily sludge from petroleum industry: a review. J. Hazard. Mater. 261, 470–490.
Ismail, A.F., Goh, P.S., Sanip, S.M., Aziz, M., 2009. Transport and separation properties of carbon nanotube-mixed matrix membrane. Sep. Purif. Technol. 70, 12–26.
Itzhak, T., Segev-Mark, N., Simon, A., Abetz, V., Ramon, G.Z., Segal-Peretz, T., 2021. Atomic layer deposition for gradient surface modification and controlled

hydrophilization of ultrafiltration polymer membranes. ACS Appl. Mater. Interfaces. 13, 15591–15600.
Kalla, S., 2021. Use of membrane distillation for oily wastewater treatment-a review. J. Environ. Chem. Eng. 9, 104641.
Kim, E.-S., Liu, Y., El-Din, M.G., 2011. The effects of pretreatment on nanofiltration and reverse osmosis membrane filtration for desalination of oil sands process-affected water. Sep. Purif. Technol. 81, 418–428.
Lapointe, M., Barbeau, B., 2020. Understanding the roles and characterizing the intrinsic properties of synthetic vs. natural polymers to improve clarification through interparticle Bridging: a review. Sep. Purif. Technol. 231, 115893.
Madwar, K., Tarazi, H., 2003. Desalination techniques for industrial wastewater reuse. Desalination 152, 325–332.
Padaki, M., Murali, R.S., Abdullah, M.S., Misdan, N., Moslehyani, A., Kassim, M.A., Hilal, N., Ismail, A.F., 2015. Membrane technology enhancement in oil - water separation . A review. Desalination 357, 197–207.
Qiao, X., Zhang, Z., Yu, J., Ye, X., 2008. Performance characteristics of a hybrid membrane pilot-scale plant for oilfield-produced wastewater. Desalination 225, 113–122.
Tummons, E.N., Chew, J.W., Fane, A.G., Tarabara, V.V., 2017. Ultrafiltration of saline oil-in-water emulsions stabilized by an anionic surfactant: effect of surfactant concentration and divalent counterions. J. Memb. Sci. 537, 384–395.
Virga, E., Parra, M.A., de Vos, W.M., 2021. Fouling of polyelectrolyte multilayer based nanofiltration membranes during produced water treatment: the role of surfactant size and chemistry. J. Colloid Interface Sci. 594, 9–19.
Vu, A., Mark, N.S., Ramon, G.Z., Qian, X., Sengupta, A., Wickramasinghe, S.R., 2019. Oil deposition on polymer brush-coated NF membranes. Membranes (Basel) 9.
Wu, J., Wei, W., Li, S., Zhong, Q., Liu, F., Zheng, J., Wang, J., 2018. The effect of membrane surface charges on demulsification and fouling resistance during emulsion separation. J. Memb. Sci. 563, 126–133.
Yu, L., Han, M., He, F., 2017. A review of treating oily wastewater. Arab. J. Chem. 10, S1913–S1922.
Zhao, C., Zhou, J., Yan, Y., Yang, L., Xing, G., Li, H., Wu, P., Wang, M., Zheng, H., 2021. Application of coagulation/flocculation in oily wastewater treatment: a review. Sci. Total Environ. 765, 142795.